

1 “Nitrogen demand, supply, and acquisition strategy control plant responses to elevated CO₂ at
2 different scales”

3

4 Evan A. Perkowski^{1*}, Ezinwanne Ezekannagha¹, Nicholas G. Smith¹

5 ¹Department of Biological Sciences, Texas Tech University, Lubbock, TX

6

7 *Corresponding author:

8 2901 Main St.

9 Lubbock, TX, 79409

10 Email: evan.a.perkowski@ttu.edu

11

12 **ORCIDs:** Evan A. Perkowski (0000-0002-9523-8892), Ezinwanne Ezekannagha (0000-0001-
13 7469-949X), Nicholas G. Smith (0000-0001-7048-4387)

14

15 **Abstract**

16 Plants respond to elevated atmospheric CO₂ concentrations by reducing photosynthetic capacity
17 – a pattern that corresponds with increased net photosynthesis, primary productivity, and growth.

18 Nitrogen availability has been hypothesized to be the primary factor controlling these responses.

19 However, recent work using eco-evolutionary optimality theory suggests that these responses are
20 driven by changes in leaf nitrogen demand to build and maintain photosynthetic enzymes, which
21 optimizes resource allocation to photosynthetic capacity and maximizes allocation to growth.

22 Here, elevated CO₂ decreased the maximum rate of Rubisco carboxylation more strongly than it
23 decreased the maximum rate of electron transport for RuBP regeneration, allowing increased net
24 photosynthesis rates to be achieved by approaching optimal coordination of Rubisco

25 carboxylation and electron transport for RuBP regeneration. Leaf photosynthetic responses to
26 elevated CO₂ were independent of nitrogen fertilization and inoculation. Increasing nitrogen
27 fertilization enhanced positive effects of elevated CO₂ on total leaf area and biomass due to

28 increased nitrogen uptake and reduced nitrogen acquisition costs. Overall, patterns expected
29 from eco-evolutionary optimality theory determined leaf photosynthetic responses to elevated
30 CO₂, while nitrogen supply constrained whole-plant responses. Findings suggest that terrestrial

31 biosphere models may improve simulations of photosynthetic processes under future novel
32 environments by adopting optimality principles.

33

34 **Keywords**

35 acclimation, eco-evolutionary optimality, growth chamber, least-cost theory, nitrogen acquisition
36 strategy, photosynthesis, plant functional ecology, whole-plant growth

37

38 **Main**

39 **Introduction**

40 Terrestrial ecosystems are regulated by complex carbon and nitrogen cycles. Terrestrial
41 biosphere models, which are beginning to include coupled carbon and nitrogen cycles^{1,2}, must
42 accurately represent these cycles under different environmental scenarios to reliably simulate
43 carbon and nitrogen fluxes^{3,4}. While the inclusion of coupled carbon and nitrogen cycles was
44 intended to improve terrestrial biosphere model reliability, the role of nitrogen availability and
45 nitrogen acquisition strategy on leaf and whole plant responses to increasing atmospheric CO₂
46 concentrations remains uncertain¹, which contributes to divergent future carbon and nitrogen flux
47 simulations across terrestrial biosphere models^{4–8}.

48 Over the past few decades, numerous studies have revealed consistent leaf and whole-
49 plant responses to elevated CO₂. At the leaf level, C₃ plants grown under elevated CO₂ exhibit
50 increased net photosynthesis rates compared to plants grown under ambient CO₂^{9–11}. These
51 patterns correspond with reduced mass- and area-based leaf nitrogen content, increased leaf mass
52 per area, reduced stomatal conductance, and reduced photosynthetic capacity, yielding increased
53 photosynthetic nitrogen-use efficiency and water-use efficiency^{9–15}. At the whole-plant level, C₃
54 plants grown under elevated CO₂ exhibit increased total leaf area, which supports greater net
55 primary productivity and total biomass compared to plants grown under ambient CO₂^{9,12,16}.

56 Despite consistent plant responses to elevated CO₂ documented across experiments,
57 mechanisms that drive these responses remain unresolved. Some have hypothesized that plant
58 responses to elevated CO₂ are constrained by nitrogen availability, as nitrogen availability limits
59 net primary productivity globally¹⁷. The progressive nitrogen limitation hypothesis predicts that
60 elevated CO₂ increases plant nitrogen uptake to support greater net primary productivity, which
61 causes nitrogen availability to decline over time¹⁸. The hypothesis predicts that this response
62 should enhance positive effects of elevated CO₂ on net primary productivity and growth under
63 elevated CO₂ over short time scales that dampen with time as nitrogen becomes progressively
64 more limiting and stored in longer-lived tissues. Growth responses to elevated CO₂ expected
65 from the progressive nitrogen limitation hypothesis have received some support from free-air
66 CO₂ enrichment experiments^{19,20}, though these patterns are not consistently observed^{21–23}.

67 Assuming positive relationships between soil nitrogen availability, leaf nitrogen content,
68 and photosynthetic capacity^{24,25}, the progressive nitrogen limitation hypothesis implies that

69 reductions in nitrogen availability over time might explain why C₃ plants grown under elevated
70 CO₂ exhibit decreased leaf nitrogen content and photosynthetic capacity. However, results from
71 free-air CO₂ enrichment experiments show that reductions in leaf nitrogen content and
72 photosynthetic capacity under elevated CO₂ are decoupled from changes in nitrogen
73 availability^{10,15,26}. Additionally, variance in leaf nitrogen and photosynthetic capacity across
74 environmental gradients may be more strongly determined through aboveground conditions that
75 set demand to build and maintain photosynthetic enzymes than soil resource availability²⁷⁻³².
76 Thus, leaf photosynthetic responses to elevated CO₂ may be a product of altered demand to build
77 and maintain photosynthetic enzymes and may not be as strongly linked to changes in nitrogen
78 availability.

79 Eco-evolutionary optimality theory provides a framework for understanding how leaf
80 photosynthetic responses to elevated CO₂ may be determined through demand to build and
81 maintain photosynthetic enzymes³³. Merging photosynthetic least-cost^{34,35} and optimal
82 coordination^{36,37} theories, eco-evolutionary optimality theory posits that reduced leaf nitrogen
83 allocation under elevated CO₂ is the downstream result of a stronger downregulation in the
84 maximum rate of Ribulose-1,5-bisphosphate (RuBP) carboxylase/oxygenase (Rubisco)
85 carboxylation (V_{cmax}) than the maximum rate of electron transport for RuBP regeneration (J_{max}),
86 which reduces leaf nitrogen demand to build and maintain photosynthetic enzymes. Optimal leaf
87 nitrogen allocation to photosynthetic capacity allows plants to make more efficient use of
88 available light while avoiding overinvestment in Rubisco, which has high nitrogen and energetic
89 costs of construction and maintenance^{24,38}. Such leaf nitrogen allocation responses to elevated
90 CO₂ increase photosynthetic nitrogen-use efficiency and allow increased net photosynthesis rates
91 to be achieved through increasingly equal co-limitation of Rubisco carboxylation and electron
92 transport for RuBP regeneration^{36,37,39,40}. The expected optimal leaf response to elevated CO₂ has
93 received some empirical support^{10,26,41,42}, though no studies have connected these patterns with
94 concurrently measured whole-plant responses.

95 The eco-evolutionary optimality hypothesis deviates from the progressive nitrogen
96 limitation hypothesis by indicating that leaf level responses to elevated CO₂ are driven by
97 changes in leaf nitrogen demand to build and maintain photosynthetic enzymes that optimize
98 resource investment to photosynthetic capacity independent of changes in soil nitrogen supply.
99 However, the eco-evolutionary optimality hypothesis does not discount the role of soil nitrogen

100 availability on whole-plant responses to elevated CO₂, where the expected optimal strategy in
101 response to elevated CO₂ is to allocate surplus nitrogen not needed to satisfy demand to build
102 and maintain photosynthetic enzymes toward the construction of a greater quantity of optimally
103 coordinated leaves and other plant organs. Thus, whether patterns expected from the progressive
104 nitrogen limitation hypothesis or eco-evolutionary optimality hypothesis control plant responses
105 to elevated CO₂ may be a matter of scale, where leaf photosynthetic responses to elevated CO₂
106 are determined through optimal resource investment to photosynthetic capacity and whole-plant
107 responses to elevated CO₂ are regulated through changes in soil nitrogen supply.

108 Plants allocate carbon belowground in exchange for nutrients through different nutrient
109 acquisition strategies, including direct uptake pathways or symbioses with mycorrhizal fungi and
110 symbiotic nitrogen-fixing bacteria. Carbon costs to acquire nitrogen, or the amount of carbon
111 plants allocate belowground per unit nitrogen acquired, vary in species with different nitrogen
112 acquisition strategies and are dependent on environmental factors such as atmospheric CO₂,
113 temperature, light availability, and nutrient availability^{43–45}. Therefore, nitrogen acquisition
114 strategy cannot be ignored when considering effects of nitrogen availability on plant responses to
115 elevated CO₂. Few studies account for acquisition strategy when considering the role of nitrogen
116 availability on leaf and whole-plant responses to elevated CO₂^{41,45}. Such studies found that
117 nitrogen acquisition strategies with reduced carbon costs to acquire nitrogen may buffer the
118 effect of nitrogen limitation at the whole-plant level⁴⁵, but leaf-level responses remain
119 inconsistent^{41,45}.

120 Here, *Glycine max* L. (Merr.) seedlings were grown under full-factorial combinations of
121 two CO₂ concentrations, two inoculation treatments, and nine soil nitrogen fertilization
122 treatments to reconcile the role of nitrogen supply and demand on plant responses to elevated
123 CO₂. We used this experimental setup to test the following hypotheses:

- 124 (1) Following the demand-driven eco-evolutionary optimality hypothesis, elevated CO₂ will
125 downregulate V_{cmax} more strongly than J_{max} , increasing $J_{\text{max}}:V_{\text{cmax}}$ and allowing increased
126 net photosynthesis rates to approach equal co-limitation of Rubisco carboxylation and
127 electron transport for RuBP regeneration. Leaf photosynthetic responses to elevated CO₂
128 will be independent of nitrogen fertilization and inoculation treatment.
- 129 (2) Following the supply-driven progressive nitrogen limitation hypothesis, positive effects
130 of elevated CO₂ on total leaf area and total biomass will be enhanced with increasing

131 nitrogen fertilization due to increased plant nitrogen uptake and reduced carbon costs to
132 acquire nitrogen. Inoculation with symbiotic nitrogen-fixing bacteria will enhance
133 positive growth responses to elevated CO₂, though these responses will only be apparent
134 under low nitrogen fertilization where individuals will invest more strongly in
135 symbiotic nitrogen fixation.

136

137 Results

138 *Leaf nitrogen content*

139 Elevated CO₂ reduced N_{area} , N_{mass} , and Chl_{area} by 29%, 50%, and 31%, respectively, and
140 increased M_{area} by 44% ($p<0.001$ in all cases; Table 1). Interactions between nitrogen
141 fertilization and CO₂ ($p<0.05$ in all cases; Table 1) indicated that positive effects of increasing
142 nitrogen fertilization on N_{area} , N_{mass} , and M_{area} ($p<0.001$ in all cases; Table 1) were stronger under
143 ambient CO₂ than elevated CO₂ (Tukey test of the nitrogen fertilization-trait slope between CO₂:
144 $p<0.05$ in all cases). These responses resulted in a stronger reduction in N_{area} and N_{mass} and a
145 stronger increase in M_{area} under elevated CO₂ with increasing nitrogen fertilization than ambient
146 CO₂ (Fig. S1). Nitrogen fertilization did not modify reductions in Chl_{area} due to elevated CO₂
147 (Tukey test of the nitrogen fertilization- Chl_{area} slope between CO₂ treatments: $p>0.05$).

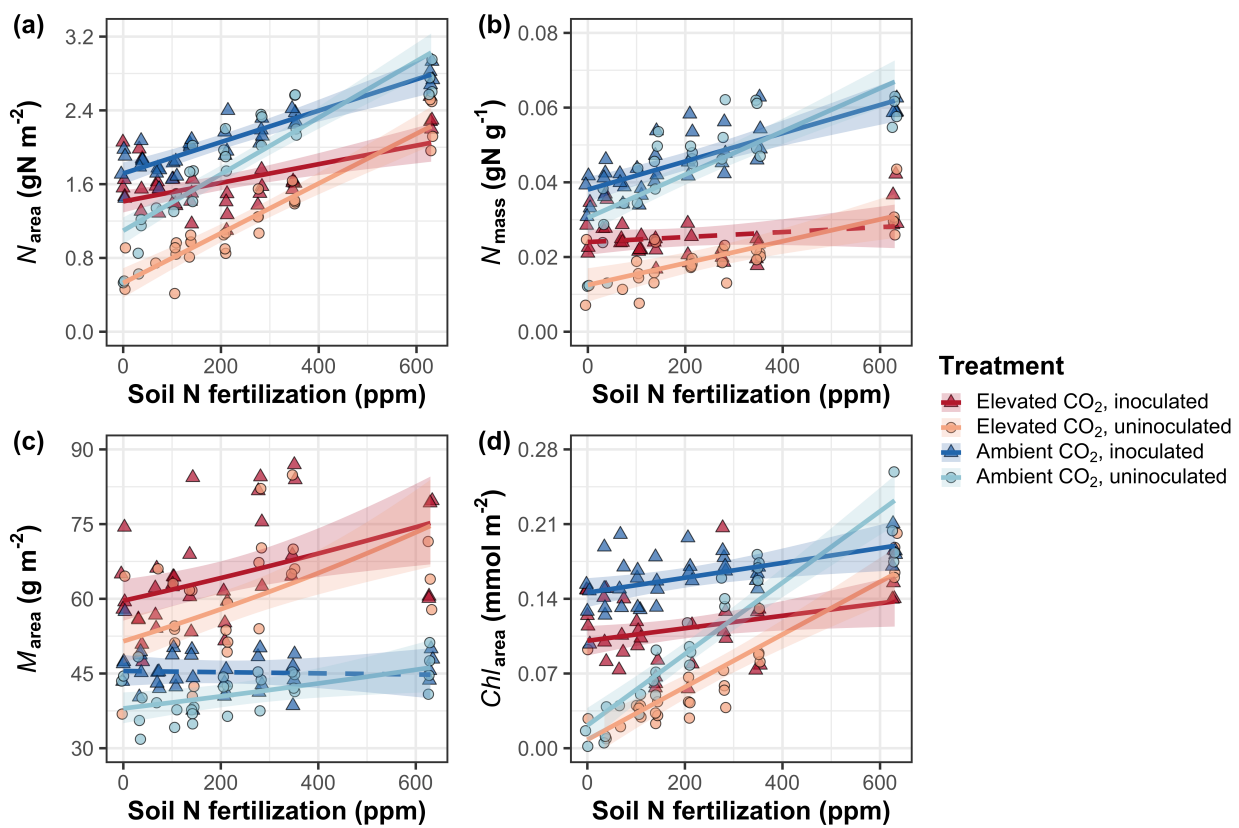
148 An interaction between inoculation and CO₂ ($p<0.05$; Table 1) indicated that reductions
149 in N_{area} due to elevated CO₂ were stronger in uninoculated plants (36% reduction; Tukey test of
150 the CO₂ effect in uninoculated plants: $p<0.001$) than inoculated plants (22% reduction; Tukey
151 test of the CO₂ effect in inoculated plants: $p<0.001$). Inoculation did not modify N_{mass} , M_{area} , or
152 Chl_{area} responses to elevated CO₂ (CO₂-by-inoculation interaction: $p>0.05$ in all cases; Table 1).
153 However, an interaction between nitrogen fertilization and inoculation ($p<0.05$ in all cases; Table
154 1; Figs. 1a-d) indicated that positive effects of increasing nitrogen fertilization on N_{area} , N_{mass} ,
155 M_{area} , and Chl_{area} ($p<0.001$ in all cases; Table 1) were stronger in uninoculated plants compared
156 to inoculated plants (Tukey test of the nitrogen fertilization-trait slope between inoculation
157 treatments: $p<0.05$ in all cases).

159 **Table 1** Effects of CO₂ concentration, inoculation, and nitrogen fertilization on leaf nitrogen allocation*

		<i>N_{area}</i>		<i>N_{mass}</i>		<i>M_{area}^a</i>		<i>Chl_{area}</i>	
	df	χ^2	<i>p</i>	χ^2	<i>p</i>	χ^2	<i>p</i>	χ^2	<i>p</i>
CO ₂	1	155.908	<0.001	272.362	<0.001	151.319	<0.001	69.233	<0.001
Inoculation (I)	1	86.029	<0.001	15.576	<0.001	19.158	<0.001	136.341	<0.001
N fertilization (N)	1	316.408	<0.001	106.659	<0.001	21.440	<0.001	163.111	<0.001
CO ₂ *I	1	4.729	0.030	2.025	0.155	0.029	0.866	2.102	0.147
CO ₂ *N	1	5.723	0.017	22.542	<0.001	7.619	0.006	2.999	0.083
I*N	1	43.381	<0.001	11.137	0.001	5.022	0.025	75.769	<0.001
CO ₂ *I*N	1	0.489	0.484	0.041	0.839	0.208	0.649	2.144	0.143

160 *Significance determined using Type II Wald χ^2 tests ($\alpha=0.05$). *P*-values less than 0.05 are in bold. A superscript “a” is included after
 161 trait labels to indicate if models were fit with natural log-transformed response variables. Key: df=degrees of freedom, χ^2 =Wald chi-
 162 square test statistic, *N_{area}*=leaf nitrogen content per unit leaf area (gN m⁻²), *N_{mass}*=leaf nitrogen content (gN g⁻¹), *M_{area}*=leaf mass per
 163 unit leaf area (g m⁻²).

164

165 **Figure 1**

166

167 **Figure 1** Effects of CO₂ concentration, nitrogen fertilization, and inoculation on leaf nitrogen per
 168 unit leaf area (a), leaf nitrogen per unit leaf mass (b), leaf mass per unit leaf area (c), and
 169 chlorophyll content per unit leaf area (d). Nitrogen fertilization is represented on the x-axis in all
 170 panels. Red shaded points and trendlines indicate plants grown under elevated CO₂, while blue
 171 shaded points and trendlines indicate plants grown under ambient CO₂. Light blue and red
 172 circular points and trendlines indicate measurements collected from uninoculated plants, while
 173 dark blue and red triangular points indicate measurements collected from inoculated plants. Solid
 174 trendlines indicate regression slopes that are different from zero ($p < 0.05$), while dashed
 175 trendlines indicate slopes that are not distinguishable from zero ($p > 0.05$).
 176

177 *Gas exchange*
178 Elevated CO₂ decreased $A_{\text{net},420}$ by 17% ($p<0.001$; Table 2) and increased $A_{\text{net,growth}}$ by 33%
179 ($p<0.001$; Table 2). Nitrogen fertilization did not modify effects of elevated CO₂ on $A_{\text{net},420}$ or
180 $A_{\text{net,growth}}$ (CO₂-by-nitrogen fertilization interaction: $p>0.05$ in both cases; Table 2; Fig. 2a-b).
181 Inoculation did not modify $A_{\text{net},420}$ responses to elevated CO₂ (CO₂-by-inoculation interaction:
182 $p>0.05$). However, an interaction between CO₂ and inoculation ($p<0.05$; Table 2) indicated that
183 inoculated plants experienced a stronger increase in $A_{\text{net,growth}}$ due to elevated CO₂ (38% increase;
184 Tukey test of the CO₂ effect in inoculated plants: $p<0.001$) compared to uninoculated plants
185 (26% increase; Tukey test of the CO₂ effect in uninoculated plants: $p<0.05$). An interaction
186 between nitrogen fertilization and inoculation ($p<0.001$ in both cases; Table 2) indicated that
187 positive effects of increasing nitrogen fertilization on $A_{\text{net},420}$ and $A_{\text{net,growth}}$ ($p<0.001$ in both
188 cases; Table 2; Fig. 2a-b) were stronger in uninoculated plants than inoculated plants (Tukey test
189 comparing the nitrogen fertilization-trait slope between inoculation treatments: $p<0.001$ in both
190 cases).

191 Elevated CO₂ decreased $V_{\text{cmax}25}$ and $J_{\text{max}25}$ by 16% and 10%, respectively, increasing
192 $J_{\text{max}25}:V_{\text{cmax}25}$ by 8% ($p<0.05$ in all cases; Table 2; Fig. 2c-e). $V_{\text{cmax}25}$, $J_{\text{max}25}$, and $J_{\text{max}25}:V_{\text{cmax}25}$
193 responses to elevated CO₂ were not modified by nitrogen fertilization (CO₂-by-nitrogen
194 fertilization interaction: $p>0.05$ in all cases; Table 2; Fig. 2c-e) or inoculation (CO₂-by-
195 inoculation interaction: $p>0.05$ in all cases; Table 2). An interaction between nitrogen
196 fertilization and inoculation ($p<0.05$ in both cases; Table 2) indicated that positive effects of
197 increasing nitrogen fertilization on $V_{\text{cmax}25}$ and $J_{\text{max}25}$ ($p<0.001$ in both cases; Table 2) and
198 negative effects of increasing nitrogen fertilization on $J_{\text{max}25}:V_{\text{cmax}25}$ ($p<0.001$; Table 2) were
199 driven by uninoculated plants (Tukey test of the nitrogen fertilization-trait slope in uninoculated
200 plants: $p<0.001$ in all cases), as there was no effect of nitrogen fertilization on $V_{\text{cmax}25}$, $J_{\text{max}25}$, or
201 $J_{\text{max}25}:V_{\text{cmax}25}$ in inoculated plants (Tukey test of the nitrogen fertilization-trait slope in inoculated
202 plants: $p>0.05$ in all cases).

203 There was no effect of CO₂ concentration on $R_{\text{d}25}$ ($p>0.05$; Table 2). An interaction
204 between nitrogen fertilization and inoculation ($p<0.001$; Table 2) indicated that the positive
205 effect of increasing nitrogen fertilization on $R_{\text{d}25}$ ($p<0.05$; Table 2) was driven by uninoculated
206 plants (Tukey test of the nitrogen fertilization- $R_{\text{d}25}$ slope in uninoculated plants: $p<0.001$), as

207 there was no effect of nitrogen fertilization on R_{d25} in inoculated plants (Tukey test of the
208 nitrogen fertilization- R_{d25} slope in inoculated plants: $p>0.05$).

209

210 *Photosynthetic nitrogen-use efficiency*

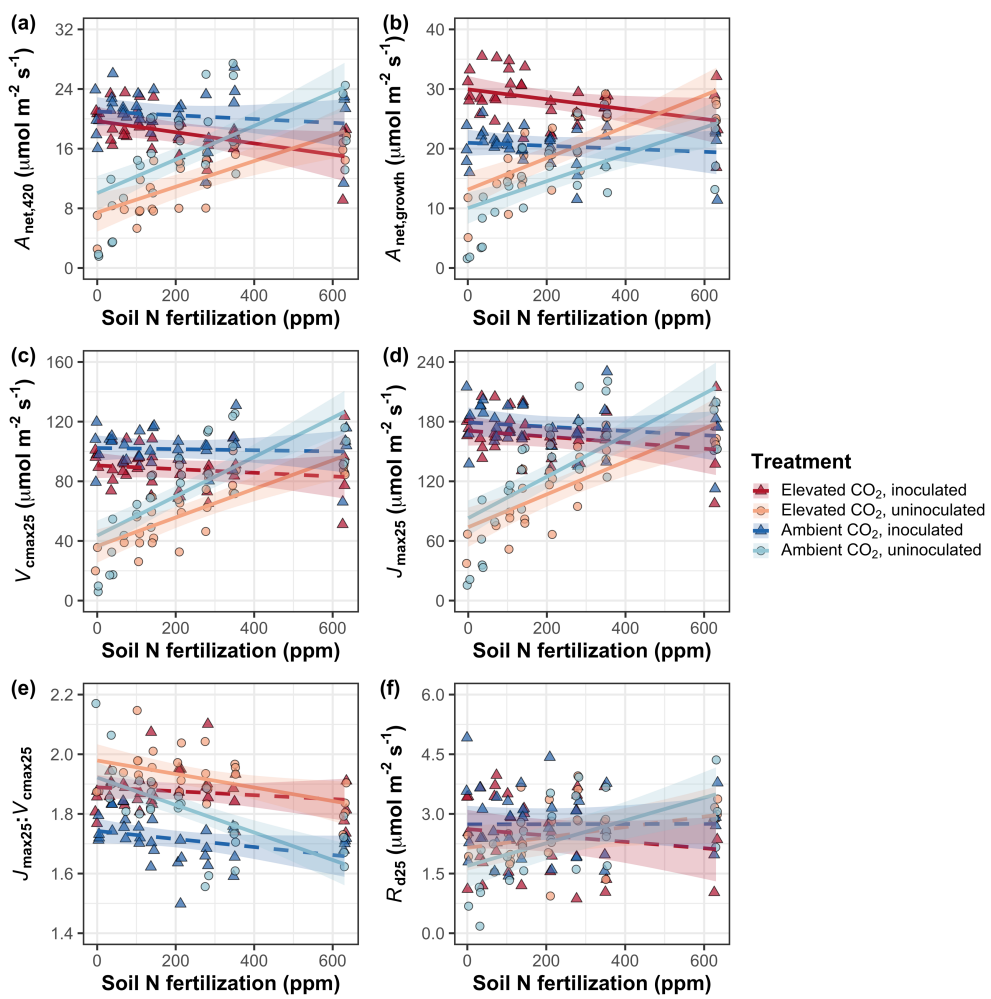
211 Elevated CO₂ increased $PNUE_{growth}$ by 90% ($p<0.001$; Table 2; Fig. 3), a pattern that was not
212 modified by inoculation treatment (CO₂-by-inoculation interaction: $p>0.05$; Table 2). An
213 interaction between CO₂ and nitrogen fertilization ($p<0.05$; Table 2) indicated that the positive
214 effect of elevated CO₂ on $PNUE_{growth}$ decreased with increasing nitrogen fertilization (Fig. S2).
215 This pattern was driven by a negative effect of increasing nitrogen fertilization on $PNUE_{growth}$
216 ($p<0.001$; Table 2) that was stronger under elevated CO₂ than ambient CO₂ (Tukey test
217 comparing the nitrogen fertilization- $PNUE_{growth}$ slope between CO₂ treatments: $p<0.05$). An
218 interaction between nitrogen fertilization and inoculation ($p<0.001$; Table 2; Fig. 3) indicated
219 that the negative effect of increasing nitrogen fertilization on $PNUE_{growth}$ was driven by
220 inoculated plants (Tukey test of the nitrogen fertilization- $PNUE_{growth}$ slope in inoculated plants:
221 $p<0.001$), as there was no effect of nitrogen fertilization on $PNUE_{growth}$ in uninoculated plants
222 (Tukey test of the nitrogen fertilization- $PNUE_{growth}$ slope in uninoculated plants: $p>0.05$).
223

224 **Table 2** Effects of CO₂ concentration, inoculation, and nitrogen fertilization on leaf gas exchange*

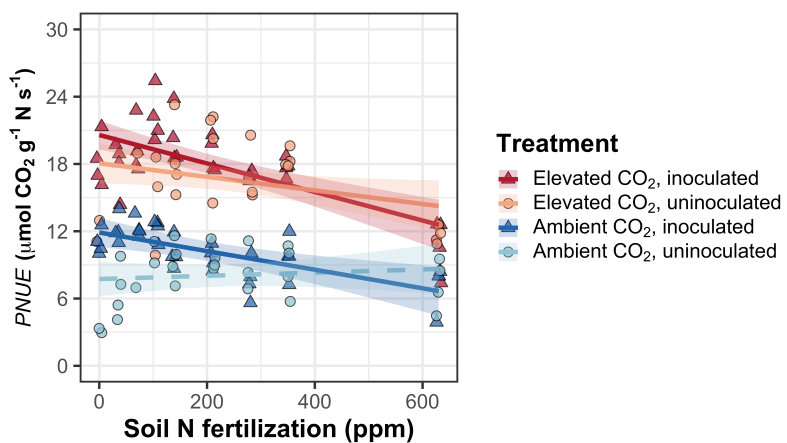
		<i>A</i> _{net,420}		<i>A</i> _{net,growth}		<i>V</i> _{cmax25}		<i>J</i> _{max25}	
	df	χ^2	<i>p</i>	χ^2	<i>p</i>	χ^2	<i>p</i>	χ^2	<i>p</i>
CO ₂	1	15.747	<0.001	52.716	<0.001	18.039	<0.001	6.042	0.014
Inoculation (I)	1	77.137	<0.001	83.008	<0.001	98.579	<0.001	85.064	<0.001
N fertilization (N)	1	11.986	<0.001	14.658	<0.001	37.053	<0.001	25.356	<0.001
CO ₂ *I	1	1.032	0.310	5.634	0.018	0.065	0.799	0.667	0.414
CO ₂ *N	1	1.998	0.158	0.135	0.713	1.758	0.185	0.742	0.389
I*N	1	46.800	<0.001	50.774	<0.001	60.394	<0.001	57.41	<0.001
CO ₂ *I*N	1	0.002	0.964	1.332	0.248	0.748	0.387	0.377	0.539

	<i>J</i> _{max25:<i>V</i>_{cmax25}}		<i>R</i> _{d25}		<i>PNUE</i> _{growth}		
	χ^2	<i>p</i>	χ^2	<i>p</i>	χ^2	<i>p</i>	
CO ₂	1	92.010	<0.001	0.256	0.613	300.197	<0.001
Inoculation (I)	1	27.768	<0.001	3.094	0.079	9.897	0.002
N fertilization (N)	1	28.147	<0.001	5.965	0.015	29.695	<0.001
CO ₂ *I	1	2.916	0.088	2.563	0.109	0.944	0.331
CO ₂ *N	1	3.210	0.073	2.675	0.102	5.359	0.021
I*N	1	9.607	0.002	12.083	0.001	10.883	<0.001
CO ₂ *I*N	1	1.102	0.294	0.244	0.622	0.369	0.544

225 *Significance determined using Type II Wald χ^2 tests ($\alpha=0.05$). *P*-values less than 0.05 are in bold. Key: df=degrees of freedom,
226 χ^2 =Wald chi-square test statistic, *A*_{net}=net photosynthesis rate ($\mu\text{mol m}^{-2} \text{s}^{-1}$), *V*_{cmax25}=maximum rate of Rubisco carboxylation at 25°C
227 ($\mu\text{mol m}^{-2} \text{s}^{-1}$), *J*_{max25}=maximum rate of electron transport for RuBP regeneration at 25°C ($\mu\text{mol m}^{-2} \text{s}^{-1}$), *J*<sub>max25:*V*_{cmax25}=ratio of *J*_{max25}
228 to *V*_{cmax25} (unitless), *R*_{d25}=dark respiration at 25°C ($\mu\text{mol m}^{-2} \text{s}^{-1}$), *PNUE*_{growth}=photosynthetic nitrogen-use efficiency ($\mu\text{mol CO}_2 \text{ gN}^{-1}$
229 s^{-1})</sub>

230 **Figure 2**

231
232 **Figure 2** Effects of CO₂, nitrogen fertilization, and inoculation on net photosynthesis measured
233 at 420 $\mu\text{mol mol}^{-1}$ CO₂ (a), net photosynthesis measured under growth CO₂ concentration (b), the
234 maximum rate of Rubisco carboxylation at 25°C (c), the maximum rate of electron transport for
235 RuBP regeneration at 25°C (d), the ratio of the maximum rate of electron transport for RuBP
236 regeneration to the maximum rate of Rubisco carboxylation (e), and dark respiration at 25°C (f).
237 Nitrogen fertilization is represented on the x-axis. Red shaded points and trendlines indicate
238 plants grown under elevated CO₂, while blue shaded points and trendlines indicate plants grown
239 under ambient CO₂. Light blue and red circular points and trendlines indicate measurements
240 collected from uninoculated plants, while dark blue and red triangular points indicate
241 measurements collected from inoculated plants. Solid trendlines indicate regression slopes that
242 are different from zero ($p < 0.05$), while dashed trendlines indicate slopes that are not
243 distinguishable from zero ($p > 0.05$).

244 **Figure 3**

245

246 **Figure 3** Effects of CO₂, nitrogen fertilization, and inoculation on photosynthetic nitrogen-use
 247 efficiency. Nitrogen fertilization is represented on the x-axis. Red shaded points and trendlines
 248 indicate plants grown under elevated CO₂, while blue shaded points and trendlines indicate
 249 plants grown under ambient CO₂. Light blue and red circular points and trendlines indicate
 250 measurements collected from uninoculated plants, while dark blue and red triangular points
 251 indicate measurements collected from inoculated plants. Solid trendlines indicate regression
 252 slopes that are different from zero ($p < 0.05$), while dashed trendlines indicate slopes that are not
 253 distinguishable from zero ($p > 0.05$).

254

255 *Whole-plant traits*
256 Elevated CO₂ increased total leaf area and total biomass by 51% and 102%, respectively
257 ($p<0.001$ in both cases; Table 3). Positive effects of elevated CO₂ on total leaf area and total
258 biomass were enhanced with increasing nitrogen fertilization (CO₂-by-nitrogen fertilization
259 interaction: $p<0.001$ in both cases; Table 3; Fig. 4a-b) but not inoculation (CO₂-by-inoculation
260 interaction: $p>0.05$ in both cases; Table 3). An interaction between nitrogen fertilization and
261 inoculation ($p<0.001$ in both cases; Table 3) indicated that positive effects of increasing nitrogen
262 fertilization on total leaf area and total biomass ($p<0.001$ in both cases; Table 3) were stronger in
263 uninoculated plants than inoculated plants (Tukey tests comparing the nitrogen fertilization-trait
264 slopes between inoculation treatments: $p<0.05$ for both traits).

265 Elevated CO₂ increased N_{cost} by 62% ($p<0.001$; Table 3), a pattern that was not modified
266 by nitrogen fertilization (CO₂-by-nitrogen fertilization interaction: $p>0.05$; Table 3). An
267 interaction between CO₂ and inoculation ($p<0.05$; Table 3) indicated that the positive effect of
268 elevated CO₂ on N_{cost} was stronger in uninoculated plants (99% increase; Tukey test evaluating
269 the CO₂ effect on N_{cost} in uninoculated plants: $p<0.001$) than inoculated plants (21% increase
270 Tukey test evaluating the CO₂ effect on N_{cost} in inoculated plants: $p<0.05$). An interaction
271 between nitrogen fertilization and inoculation ($p<0.001$; Table 3) indicated that the negative
272 effect of increasing nitrogen fertilization on N_{cost} ($p<0.001$; Table 3) was stronger in
273 uninoculated plants (Tukey test comparing the nitrogen fertilization- N_{cost} slope between
274 inoculation treatments: $p<0.001$). A three-way interaction ($p<0.001$; Table 3) indicated that
275 interactions between nitrogen fertilization and inoculation were stronger under elevated CO₂ than
276 ambient CO₂. This pattern was driven by greater N_{cost} in uninoculated plants grown under
277 elevated CO₂ and low nitrogen fertilization than any other CO₂-by-inoculation treatment
278 combination under low nitrogen fertilization (Tukey test comparing N_{cost} in uninoculated
279 individuals grown under elevated CO₂ and 0 ppm N to all other CO₂-inoculation treatment
280 combinations grown under 0 ppm N: $p<0.001$ in all cases; Fig. 4c). N_{cost} was generally reduced
281 in inoculated plants ($p<0.001$; Table 3).

282
283 *Nitrogen fixation*
284 There was no effect of CO₂ concentration on % N_{dfa} ($p=0.472$; Table 3; Fig. 4d). An interaction
285 between nitrogen fertilization and inoculation ($p<0.001$; Table 3) indicated that the negative

286 effect of increasing nitrogen fertilization on $\%N_{dfa}$ ($p<0.001$; Table 3) was driven by inoculated
287 plants (Tukey test of the nitrogen fertilization- $\%N_{dfa}$ slope in inoculated plants: $p<0.001$), as
288 there was no effect of nitrogen fertilization on $\%N_{dfa}$ in uninoculated plants (Tukey test of the
289 nitrogen fertilization- $\%N_{dfa}$ slope in uninoculated plants: $p>0.05$; Fig. 4d).

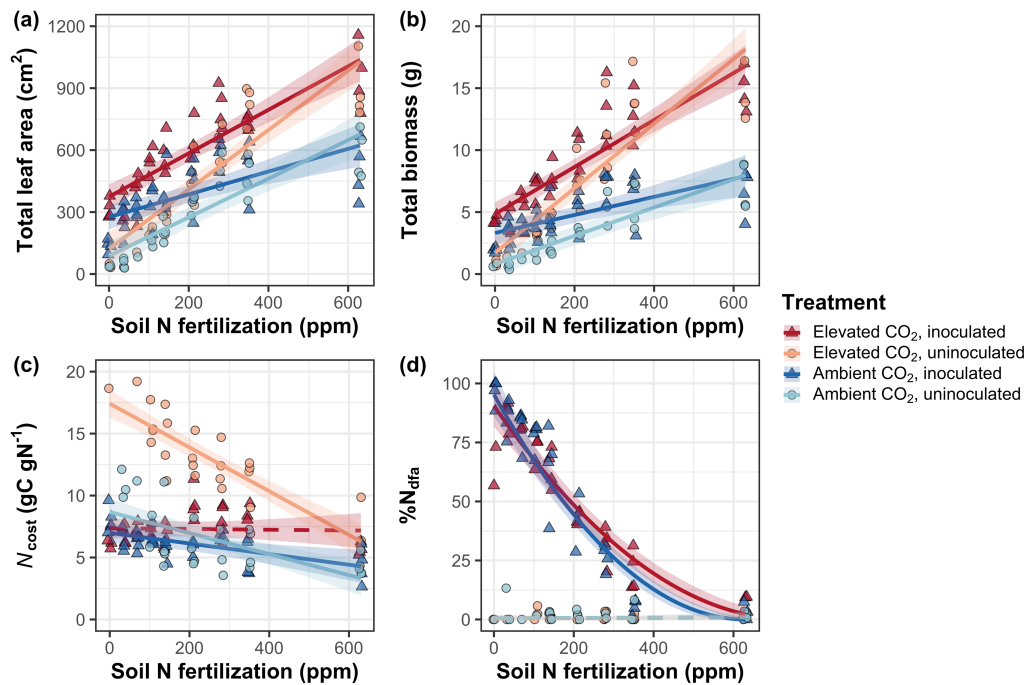
290

291 **Table 3** Effects of CO₂ concentration, inoculation, and nitrogen fertilization on whole-plant growth, carbon costs to acquire nitrogen,
 292 and investment toward symbiotic nitrogen fixation*

		Total leaf area		Total biomass ^b		Carbon cost to acquire nitrogen		%N _{dfa} ^b	
	df	χ^2	p	χ^2	p	χ^2	p	χ^2	p
CO ₂	1	69.291	<0.001	131.477	<0.001	88.189	<0.001	0.518	0.472
Inoculation (I)	1	35.715	<0.001	34.264	<0.001	136.343	<0.001	955.57	<0.001
N fertilization (N)	1	274.199	<0.001	269.046	<0.001	80.501	<0.001	292.938	<0.001
CO ₂ *I	1	2.064	0.151	0.518	0.472	85.237	<0.001	2.010	0.156
CO ₂ *N	1	18.655	<0.001	16.877	<0.001	1.050	0.306	2.716	0.099
I*N	1	10.804	0.001	15.779	<0.001	46.489	<0.001	231.29	<0.001
CO ₂ *I*N	1	<0.001	0.990	0.023	0.880	18.125	<0.001	2.119	0.145

293 *Significance determined using Type II Wald χ^2 tests ($\alpha=0.05$). P-values less than 0.05 are in bold. A superscript “^b” after trait labels
 294 indicates if models were fit using square root transformed variables. Key: df=degrees of freedom, χ^2 =Wald chi-square test statistic,
 295 total leaf area (cm²), total biomass (g), carbon cost to acquire nitrogen (gC gN⁻¹), %N_{dfa}=percent leaf nitrogen content fixed from the
 296 atmosphere (%).

297

298 **Figure 4**

299

300 **Figure 4.** Effects of CO₂, nitrogen fertilization, and inoculation on total leaf area (a), total
 301 biomass (b), structural carbon costs to acquire nitrogen (c), and percent of leaf nitrogen content
 302 derived from the atmosphere (d). Nitrogen fertilization is represented on the x-axis. Red shaded
 303 points and trendlines indicate plants grown under elevated CO₂, while blue shaded points and
 304 trendlines indicate plants grown under ambient CO₂. Light blue and red circular points and
 305 trendlines indicate measurements collected from uninoculated plants, while dark blue and red
 306 triangular points indicate measurements collected from inoculated plants. Solid trendlines
 307 indicate regression slopes that are different from zero ($p < 0.05$), while dashed trendlines indicate
 308 slopes that are not distinguishable from zero ($p > 0.05$).
 309

310 **Discussion**

311 *Glycine max* seedlings were grown under two CO₂ concentrations, two inoculation treatments,
312 and nine soil nitrogen fertilization treatments in a full-factorial growth chamber experiment to
313 reconcile the role of nitrogen supply, demand, and acquisition strategy on leaf and whole-plant
314 responses to elevated CO₂.

315 Results revealed that elevated CO₂ increased $A_{\text{net,growth}}$ despite reduced N_{area} , V_{cmax25} , and
316 J_{max25} . Larger reductions in V_{cmax25} than J_{max25} increased $J_{\text{max25}}:V_{\text{cmax25}}$, while respective increases
317 and decreases in $A_{\text{net,growth}}$ and N_{area} increased photosynthetic nitrogen-use efficiency. These
318 patterns are consistent with previous studies that have investigated or reviewed leaf responses to
319 elevated CO₂^{9–12,14,16,26,46}. Positive effects of elevated CO₂ on $A_{\text{net,growth}}$ and $J_{\text{max25}}:V_{\text{cmax25}}$ and
320 negative effects of elevated CO₂ on V_{cmax25} and J_{max25} were not related to nitrogen supply.
321 However, increased $J_{\text{max25}}:V_{\text{cmax25}}$ and photosynthetic nitrogen-use efficiency provide strong
322 support for the idea that leaves were downregulating V_{cmax25} in response to elevated CO₂ such
323 that enhanced net photosynthesis rates approached optimal coordination of Rubisco
324 carboxylation and electron transport for RuBP regeneration^{36,37,41}. Photosynthetic responses to
325 elevated CO₂ decreased demand to build and maintain photosynthetic enzymes and were not
326 modified across the nitrogen fertilization gradient, following patterns expected from eco-
327 evolutionary optimality theory^{33,41,42}.

328 Leaf photosynthetic responses to elevated CO₂ corresponded with increased total leaf
329 area and total biomass, patterns that are also consistent with previous studies that have
330 investigated or reviewed whole-plant responses to elevated CO₂^{9,11,16,46}. Greater whole-plant
331 growth under elevated CO₂ was associated with greater carbon costs to acquire nitrogen through
332 stronger increases in belowground carbon allocation than whole-plant nitrogen uptake, indicating
333 that plants grown under elevated CO₂ supported greater total leaf area and total biomass through
334 increased plant nitrogen uptake, though at reduced nitrogen uptake efficiency.

335 Unlike leaf photosynthetic responses, positive whole-plant responses to elevated CO₂
336 were enhanced with increasing nitrogen fertilization, supporting our hypothesis that nitrogen
337 supply would constrain whole-plant responses to elevated CO₂. Positive effects of increasing
338 nitrogen fertilization on total leaf area and total biomass were associated with reductions in
339 carbon costs to acquire nitrogen, a pattern that was driven by stronger increases in whole-plant
340 nitrogen uptake than belowground carbon allocation⁴⁴. While reductions in carbon costs to

341 acquire nitrogen due to increasing nitrogen fertilization were similar between CO₂ treatments,
342 increasing nitrogen fertilization increased whole-plant nitrogen uptake more strongly under
343 elevated CO₂. This pattern, coupled with similar effects of nitrogen fertilization on belowground
344 carbon allocation responses to elevated CO₂, indicated that stronger growth responses to elevated
345 CO₂ with increasing nitrogen fertilization were likely driven by enhanced nitrogen uptake
346 efficiency. These findings suggest that positive short-term effects of nitrogen supply on whole-
347 plant responses to elevated CO₂ are linked to reduced costs of acquiring nitrogen and increased
348 nitrogen uptake efficiency, supporting previous results⁴⁵.

349 Nitrogen supply and demand could each explain plant responses to elevated CO₂, though
350 these factors operated at different scales. Specifically, photosynthetic responses to elevated CO₂
351 reduced leaf nitrogen demand to build and maintain photosynthetic enzymes, which increased
352 photosynthetic nitrogen-use efficiency and allowed increased net photosynthesis rates to
353 approach optimal coordination of Rubisco carboxylation and electron transport for RuBP
354 regeneration^{36,37}. Whole-plant responses to elevated CO₂ were enhanced with increasing soil
355 nitrogen supply. Interestingly, optimized nitrogen allocation to photosynthetic capacity may have
356 resulted in nitrogen savings at the leaf level that could have maximized nitrogen allocation to
357 growth. These results suggest that plants grown under elevated CO₂ responded to increased
358 nitrogen supply by increasing the number of optimally coordinated leaves and that the
359 downregulation in photosynthetic capacity under elevated CO₂ was not a direct response to
360 changes in nitrogen supply.

361 Inoculation increased N_{area} , $A_{\text{net},420}$, $A_{\text{net,growth}}$, $V_{\text{cmax}25}$, $J_{\text{max}25}$, photosynthetic nitrogen-use
362 efficiency, total leaf area, and total biomass, and decreased $J_{\text{max}25}:V_{\text{cmax}25}$ and $R_{\text{d}25}$. These patterns
363 support previous literature suggesting that species that form associations with symbiotic
364 nitrogen-fixing bacteria have increased leaf nitrogen content, photosynthetic capacity, and
365 growth compared to species that do not form such associations^{47,48}. Positive effects of
366 inoculation on leaf and whole-plant traits were strongest under low nitrogen fertilization and
367 rapidly diminished with increasing nitrogen fertilization as investment in symbiotic nitrogen
368 fixation decreased, supporting the idea that nitrogen fixation is a nutrient acquisition strategy that
369 may confer competitive benefits for nitrogen-fixing species growing in low soil nitrogen
370 environments^{49–51}.

371 Interestingly, inoculation did not modify effects of elevated CO₂ on V_{cmax25} , J_{max25} ,
372 $J_{max25} \cdot V_{cmax25}$, photosynthetic nitrogen-use efficiency, total leaf area, or total biomass. These
373 patterns corresponded with null effects of elevated CO₂ on % N_{dfa} and the ratio of root nodule
374 biomass to root biomass, suggesting that null inoculation effects on plant responses to elevated
375 CO₂ were primarily due to similar plant investments toward symbiotic nitrogen fixation between
376 CO₂ treatments. We observed these patterns regardless of nitrogen fertilization level, contrasting
377 our hypothesis that inoculation would enhance whole-plant responses to elevated CO₂ under low
378 nitrogen fertilization where individuals were expected to be invested more strongly in symbiotic
379 nitrogen fixation. These patterns contrast previous work showing that plant investment toward
380 symbiotic nitrogen fixation tends to be greater under scenarios that increase whole-plant demand
381 to acquire nitrogen^{44,51–53}. Interestingly, stronger positive effects of elevated CO₂ on $A_{net,growth}$ in
382 inoculated individuals support previously observed patterns¹⁶, though this response was not due
383 to alterations in plant investment toward the rhizobial symbiosis.

384 Many terrestrial biosphere models predict photosynthetic capacity through parameterized
385 relationships between N_{area} and V_{cmax} ^{46,54}, which assumes that leaf nitrogen-photosynthesis
386 relationships are constant across growing environments. Our results build on previous work
387 suggesting that leaf nitrogen-photosynthesis relationships dynamically change across growing
388 environments^{32,55}, as elevated CO₂ reduced leaf nitrogen content more strongly than it increased
389 $A_{net,growth}$ and decreased V_{cmax25} and J_{max25} . Additionally, positive effects of increasing nitrogen
390 fertilization on indices of photosynthetic capacity were only apparent in uninoculated plants, as
391 there was no effect of nitrogen fertilization on V_{cmax25} or J_{max25} in inoculated plants. Positive
392 effects of increasing nitrogen fertilization on N_{area} and Chl_{area} were also markedly weaker in
393 inoculated plants compared to uninoculated plants. These patterns indicate that leaf nitrogen-
394 photosynthesis relationships are context-dependent on nitrogen acquisition strategy, may only be
395 constant in environments where nitrogen supply limits leaf physiology, and will likely shift in
396 response to increasing atmospheric CO₂ concentrations. Terrestrial biosphere models that predict
397 photosynthetic capacity through parameterized relationships between N_{area} and V_{cmax} ^{56,57} may risk
398 overestimating photosynthetic capacity, therefore net primary productivity and the magnitude of
399 the land carbon sink, under future novel growth environments.

400 Our results demonstrate that optimal resource allocation to photosynthetic capacity
401 defines leaf photosynthetic responses to elevated CO₂ and that these responses are independent

402 of nitrogen supply. Current approaches for simulating photosynthetic responses to CO₂ in
403 terrestrial biosphere models with coupled carbon and nitrogen cycles often invoke patterns
404 expected from progressive nitrogen limitation, where photosynthetic responses to elevated CO₂
405 are modeled as a function of positive relationships between nitrogen availability and leaf
406 nitrogen content. Findings presented here contradict this framework, suggesting that leaf
407 photosynthetic responses to elevated CO₂ result in optimized nitrogen allocation to satisfy
408 reduced leaf nitrogen demand to build and maintain photosynthetic enzymes. Optimality models
409 that use principles from optimal coordination and photosynthetic least-cost theories are capable
410 of capturing photosynthetic responses to CO₂ independent of nitrogen supply^{33,41}, suggesting that
411 including optimality frameworks in terrestrial biosphere models may improve the accuracy by
412 which models simulate photosynthetic processes in response to increasing atmospheric CO₂
413 concentrations.

414 Previous work has highlighted that pot experiments restrict belowground rooting volume
415 and therefore may alter plant allocation responses to environmental change^{16,58}. In this study, the
416 ratio of pot volume to total biomass was greater under elevated CO₂ and increased with
417 increasing nitrogen fertilization such that several treatment combinations exceeded values
418 recommended to avoid growth limitation imposed by restricted pot volume (<1 g L⁻¹; Table S6;
419 Fig. S6)⁵⁸. We found no apparent saturating effect of increasing fertilization on total biomass,
420 belowground carbon biomass, or root biomass under conditions where biomass: pot volume
421 ratios exceeded 1 g L⁻¹ (e.g., individuals of either inoculation status grown under high
422 fertilization and elevated CO₂), which might be expected if pot volume had limited plant growth.
423 Additionally, similar responses to elevated CO₂ have been observed using field measurements
424 that do not restrict belowground rooting volume^{10,15,26,41}. The lack of such saturating responses
425 combined with similar field observations indicate that the pot volume used in this study (6 L)
426 was likely sufficient to avoid growth limitation.

427 Overall, results reported here indicate that nitrogen supply and demand each helped
428 explain *G. max* responses to elevated CO₂, though operated at different scales. Supporting eco-
429 evolutionary optimality theory, leaf photosynthetic responses to elevated CO₂ were independent
430 of soil nitrogen supply and, in most cases, inoculation. Instead, elevated CO₂ decreased leaf
431 nitrogen demand to build and maintain photosynthetic enzymes, allowing net photosynthesis
432 rates to approach equal co-limitation of Rubisco-limited and electron transport for RuBP

433 regeneration-limited photosynthesis through optimized leaf nitrogen allocation to photosynthetic
434 enzymes. Supporting the progressive nitrogen limitation hypothesis, whole-plant responses to
435 elevated CO₂ were enhanced with increasing nitrogen fertilization due to increased plant nitrogen
436 uptake efficiency coupled with possible cascading effects of nitrogen savings at the leaf level
437 that may have maximized nitrogen allocation to whole-plant growth. Inoculation did not modify
438 whole-plant responses to elevated CO₂, as plants invested similarly in symbiotic nitrogen
439 fixation between CO₂ treatments. These results suggest that plants grown under elevated CO₂
440 responded to increased nitrogen supply by increasing the number of optimally coordinated leaves
441 and that the downregulation in photosynthetic capacity under elevated CO₂ was not modified by
442 changes in nitrogen supply. The differential role of nitrogen supply on leaf and whole-plant
443 responses to elevated CO₂, coupled with dynamic leaf nitrogen-photosynthesis relationships
444 across CO₂ and nitrogen fertilization treatments, suggests that terrestrial biosphere models may
445 improve simulations of photosynthetic responses to increasing atmospheric CO₂ concentrations
446 by adopting frameworks that include optimality principles.

447

448 **Methods**

449 *Seed treatments and experimental design*

450 *Glycine max* seeds were planted in 144 6-liter surface sterilized pots (NS-600, Nursery Supplies,
451 Orange, CA, USA) containing a steam-sterilized 70:30 volume: volume mix of *Sphagnum* peat
452 moss (Premier Horticulture, Quakertown, PA, USA) to sand (Pavestone, Atlanta, GA, USA).
453 Before planting, all *G. max* seeds were surface sterilized in 2% sodium hypochlorite for 3
454 minutes, followed by three separate 3-minute washes with ultrapure water (MilliQ 7000;
455 MilliporeSigma, Burlington, MA USA). Subsets of surface-sterilized seeds were inoculated with
456 *Bradyrhizobium japonicum* (Verdesian N-Dure™ Soybean, Cary, NC, USA) in a slurry
457 following manufacturer recommendations.

458 Seventy-two pots were randomly planted with surface-sterilized seeds inoculated with *B.*
459 *japonicum*, while the remaining 72 pots were planted with surface-sterilized uninoculated seeds.
460 Thirty-six pots in each inoculation treatment were placed in one of two atmospheric CO₂
461 treatments (420, 1000 µmol mol⁻¹ CO₂). Plants in each unique inoculation-by-CO₂ treatment
462 combination received one of nine nitrogen fertilization treatments equivalent to 0 (0 mM), 35
463 (2.5 mM), 70 (5 mM), 105 (7.5 mM), 140 (10 mM), 210 (15 mM), 280 (20 mM), 350 (25 mM),

464 or 630 ppm (45 mM) N. Nitrogen fertilization treatments were created using a modified
465 Hoagland's solution⁵⁹ designed to keep concentrations of all other macronutrients and
466 micronutrients equivalent across treatments (Table S1). Plants received the same nitrogen
467 fertilization treatment twice per week in 150 mL doses as topical agents to the soil surface.

468

469 *Growth chamber conditions*

470 Plants were randomly placed in one of six Percival LED-41L2 growth chambers (Percival
471 Scientific Inc., Perry, IA, USA) over two experimental iterations due to chamber space
472 limitation. Two iterations were conducted such that one iteration included all plants grown under
473 elevated CO₂, and the second iteration included all plants grown under ambient CO₂. Average (\pm
474 SD) CO₂ concentrations across chambers throughout the experiment were 439 \pm 5 $\mu\text{mol mol}^{-1}$
475 CO₂ for the ambient treatment and 989 \pm 4 $\mu\text{mol mol}^{-1}$ CO₂ for the elevated treatment.

476 Daytime growth conditions were simulated using a 16-hour photoperiod, with incoming
477 light radiation set to chamber maximum (mean \pm SD: 1230 \pm 12 $\mu\text{mol m}^{-2} \text{s}^{-1}$ across chambers), air
478 temperature set to 25°C, and relative humidity set to 50%. The remaining 8-hour period
479 simulated nighttime growing conditions, with incoming light radiation set to 0 $\mu\text{mol m}^{-2} \text{s}^{-1}$,
480 chamber temperature set to 17°C, and relative humidity set to 50%. Transitions between daytime
481 and nighttime growing conditions were simulated by ramping incoming light radiation in 45-
482 minute increments and temperature in 90-minute increments over a 3-hour period (Table S2).

483 Plants grew under average (\pm SD) daytime light intensity of 1049 \pm 27 $\mu\text{mol m}^{-2} \text{s}^{-1}$,
484 including ramping periods. In the elevated CO₂ iteration, plants grew under 24.0 \pm 0.2°C during
485 the day, 16.4 \pm 0.8°C during the night, and 51.6 \pm 0.4% relative humidity. In the ambient CO₂
486 iteration, plants grew under 23.9 \pm 0.2°C during the day, 16.0 \pm 1.4°C during the night, and
487 50.3 \pm 0.2% relative humidity. Any differences in climate conditions across the six chambers were
488 accounted for by shuffling the same group of plants throughout the growth chambers. This
489 process was done by iteratively moving the group of plants on the top rack of a chamber to the
490 bottom rack of the same chamber, while simultaneously moving the group of plants on the
491 bottom rack of a chamber to the top rack of the adjacent chamber. Plants were moved within and
492 across chambers daily during each experiment iteration.

493

494 *Leaf gas exchange measurements*

Leaf gas exchange measurements were collected on the seventh week of development, before the onset of reproduction. All gas exchange measurements were collected on the center leaf of the most recent fully expanded trifoliate leaf set using LI-6800 portable photosynthesis machines configured with a 6800-01A fluorometer head and 6 cm² aperture (LI-COR Biosciences, Lincoln, NE, USA). Specifically, net photosynthesis (A_{net} ; $\mu\text{mol m}^{-2} \text{s}^{-1}$), stomatal conductance (g_{sw} ; $\text{mol m}^{-2} \text{s}^{-1}$), and intercellular CO₂ (C_i ; $\mu\text{mol mol}^{-1}$) concentrations were measured across a range of atmospheric CO₂ concentrations (i.e., an A_{net}/C_i curve) using the Dynamic Assimilation™ Technique. The Dynamic Assimilation™ Technique corresponds well with traditional steady-state A_{net}/C_i curves in *G. max*⁶⁰. A_{net}/C_i curves were generated along a reference CO₂ ramp down from 420 $\mu\text{mol mol}^{-1}$ CO₂ to 20 $\mu\text{mol mol}^{-1}$ CO₂, followed by a ramp up from 420 $\mu\text{mol mol}^{-1}$ CO₂ to 1620 $\mu\text{mol mol}^{-1}$ CO₂ after a 90-second wait period at 420 $\mu\text{mol mol}^{-1}$ CO₂. The ramp rate for each curve was set to 200 $\mu\text{mol mol}^{-1} \text{min}^{-1}$, logging every five seconds, generating 96 data points per response curve. All A_{net}/C_i curves were conducted after A_{net} and g_{sw} stabilized in a LI-6800 cuvette set to a 500 mol s⁻¹ flow rate, 10000 rpm mixing fan speed, 1.5 kPa vapor pressure deficit, 25°C leaf temperature, 2000 $\mu\text{mol m}^{-2} \text{s}^{-1}$ incoming light radiation, and initial reference CO₂ set to 420 $\mu\text{mol mol}^{-1}$.

Snapshot A_{net} measurements were extracted from each A_{net}/C_i curve, both at a common CO₂ concentration, 420 $\mu\text{mol mol}^{-1}$ CO₂ ($A_{\text{net},420}$; $\mu\text{mol m}^{-2} \text{s}^{-1}$), and growth CO₂ concentration, 420 and 1000 $\mu\text{mol mol}^{-1}$ CO₂ ($A_{\text{net,growth}}$; $\mu\text{mol m}^{-2} \text{s}^{-1}$). Dark respiration (R_d ; $\mu\text{mol m}^{-2} \text{s}^{-1}$) measurements were collected on the same leaf used to generate A_{net}/C_i curves following at least 30 minutes of darkness. Measurements were collected on a 5-second log interval for 60 seconds after the leaf stabilized in a LI-6800 cuvette set to a 500 mol s⁻¹ flow rate, 10000 rpm mixing fan speed, 1.5 kPa vapor pressure deficit, 25°C leaf temperature, and 420 $\mu\text{mol mol}^{-1}$ reference CO₂ concentration (regardless of CO₂ treatment), with incoming light radiation set to 0 $\mu\text{mol m}^{-2} \text{s}^{-1}$. A single dark respiration value was determined for each leaf by calculating the mean dark respiration value across the logging interval.

A/C_i curve-fitting and parameter estimation
 A_{net}/C_i curves were fit using the ‘fitaci’ function in the ‘plantecophys’ R package⁶¹. This function estimates the maximum rate of Rubisco carboxylation (V_{cmax} ; $\mu\text{mol m}^{-2} \text{s}^{-1}$) and maximum rate of electron transport for RuBP regeneration (J_{max} ; $\mu\text{mol m}^{-2} \text{s}^{-1}$) based on the Farquhar *et al.* (1980)

biochemical model of C₃ photosynthesis⁶². Triose phosphate utilization (TPU) limitation was included as an additional rate-limiting step after visually observing clear TPU limitation for most curves. All curve fits included measured dark respiration values. As A_{net}/C_i curves were generated using a common leaf temperature (25°C), curves were fit using Michaelis-Menten coefficients for Rubisco affinity to CO₂ (K_c ; μmol mol⁻¹) and O₂ (K_o ; mmol mol⁻¹), and the CO₂ compensation point (I^* ; μmol mol⁻¹) reported in⁶³. Specifically, K_c was set to 404.9 μmol mol⁻¹, K_o was set to 278.4 μmol mol⁻¹, and I^* was set to 42.75 μmol mol⁻¹. V_{cmax} , J_{max} , and R_d estimates are referenced throughout the rest of the paper as $V_{\text{cmax}25}$, $J_{\text{max}25}$, and R_{d25} .

534

535 *Leaf trait measurements*

The leaf used to generate A_{net}/C_i curves and dark respiration measurements was harvested immediately following gas exchange measurements. Images of each focal leaf were curated using a flat-bed scanner to determine fresh leaf area using the 'LeafArea' R package⁶⁴, which automates leaf area calculations using ImageJ software. Post-processed images were visually assessed to check against errors in the automation process. Each leaf was dried at 65°C for at least 48 hours and weighed and ground until homogenized. Leaf mass per area (M_{area} ; g m⁻²) was calculated as the ratio of dry leaf biomass to fresh leaf area. Leaf nitrogen content (N_{mass} ; gN g⁻¹) was quantified using a subsample of ground and homogenized leaf tissue through elemental combustion (Costech-4010, Costech, Inc., Valencia, CA, USA). Leaf nitrogen content per unit leaf area (N_{area} ; gN m⁻²) was calculated by multiplying N_{mass} and M_{area} . Photosynthetic nitrogen-use efficiency ($PNUE_{\text{growth}}$; μmol CO₂ g⁻¹ N s⁻¹) was estimated as the ratio of $A_{\text{net,growth}}$ to N_{area} .

Chlorophyll content was extracted from a second leaf in the same trifoliate leaf set as the leaf used to generate A_{net}/C_i curves. A cork borer was used to punch between 3-5 0.6 cm² disks from the leaf. Images of each set of leaf disks were curated using a flat-bed scanner to determine wet leaf area, again quantified using the 'LeafArea' R package⁶⁴. Leaf disks were shuttled into a test tube containing 10 mL dimethyl sulfoxide, vortexed, and incubated at 65°C for 120 minutes⁶⁵. Incubated test tubes were vortexed again before being loaded in 150 μL triplicate aliquots to a 96-well plate. Dimethyl sulfoxide was loaded in each plate as a single 150 μL triplicate aliquot and used as a blank. Absorbance measurements at 649 nm (A_{649}) and 665 nm (A_{665}) were recorded using a plate reader (Biotek Synergy H1; Biotek Instruments, Winooski, VT USA), with triplicate measurements averaged and corrected by the mean of the blank absorbance

557 value. Blank-corrected absorbance values were used to estimate Chl_a ($\mu\text{g mL}^{-1}$) and Chl_b ($\mu\text{g mL}^{-1}$) following equations from⁶⁶:

559 $Chl_a = 12.47A_{665} - 3.62A_{649}$ (1)

560 and

561 $Chl_b = 25.06A_{649} - 6.5A_{665}$ (2)

562 Chl_a and Chl_b were converted to mmol mL^{-1} using the molar masses of chlorophyll *a* (893.51 g mol⁻¹) and chlorophyll *b* (907.47 g mol⁻¹), then added together to calculate the total chlorophyll content in dimethyl sulfoxide extractant (mmol mL^{-1}). Total chlorophyll content (mmol) was determined by multiplying the total chlorophyll content in dimethyl sulfoxide by the volume of dimethyl sulfoxide extractant (10 mL). Area-based chlorophyll content (Chl_{area} ; mmol m^{-2}) was then calculated by dividing the total chlorophyll content by the total area of the leaf disks.

568 Subsamples of ground and homogenized leaf tissue were sent to the University of California-Davis Stable Isotope Facility to determine leaf $\delta^{13}\text{C}$ and $\delta^{15}\text{N}$ using an elemental analyzer (Elementar vario MICRO cube elemental analyzer; Elementar Analysensysteme GmbH, Langenselbold, Germany) interfaced to an isotope ratio mass spectrometer (PDZ Europa 20-20 Isotope Ratio Mass Spectrometer, Sercon Ltd., Cheshire, UK). Leaf $\delta^{13}\text{C}$ was used to estimate the time-integrated ratio of leaf intercellular CO_2 concentration to atmospheric CO_2 concentration (χ , unitless), summarized in the *Supplemental Material*. The percent of leaf nitrogen acquired from the atmosphere (% N_{dfa} ; %) was estimated using leaf $\delta^{15}\text{N}$ and the following equation⁵⁰:

577
$$\%N_{dfa} = \frac{\delta^{15}\text{N}_{direct} - \delta^{15}\text{N}_{sample}}{\delta^{15}\text{N}_{direct} - \delta^{15}\text{N}_{fixation}}$$
 (3)

578 where $\delta^{15}\text{N}_{direct}$ refers to $\delta^{15}\text{N}$ from plants that acquired nitrogen only through direct uptake, 579 $\delta^{15}\text{N}_{sample}$ refers to an individual's leaf $\delta^{15}\text{N}$, and $\delta^{15}\text{N}_{fixation}$ refers to $\delta^{15}\text{N}$ from individuals 580 entirely reliant on nitrogen fixation. $\delta^{15}\text{N}_{direct}$ was calculated as the mean leaf $\delta^{15}\text{N}$ of 581 uninoculated individuals for each nitrogen fertilization-by- CO_2 treatment combination. Any 582 individual with visual evidence of root nodule formation or nodule initiation was omitted from 583 $\delta^{15}\text{N}_{direct}$. $\delta^{15}\text{N}_{fixation}$ was calculated for each CO_2 treatment using the mean leaf $\delta^{15}\text{N}$ of 584 inoculated individuals that received 0 ppm N. $\delta^{15}\text{N}_{fixation}$ was not calculated for each nitrogen 585 fertilization-by- CO_2 treatment combination due to decreased reliance on symbiotic nitrogen 586 fixation with increasing nitrogen fertilization^{44,49,50}.

587

588 *Whole-plant measurements*

589 All individuals were harvested, and biomass of major organ types (leaves, stems, roots, and
590 nodules when present) were separated immediately following gas exchange measurements. Fresh
591 leaf area of all harvested leaves was measured using a LI-3100C (LI-COR Biosciences, Lincoln,
592 Nebraska, USA). Total fresh leaf area (cm^2) was calculated as the sum of all leaf areas, including
593 the leaf used for gas exchange and chlorophyll extractions. Harvested material was separately
594 dried in an oven set to 65°C for at least 48 hours to a constant mass, weighed, and ground to
595 homogeneity. Leaves and root nodules were ground using a mortar and pestle, while stems and
596 roots were ground using an E3300 Single Speed Mini Cutting Mill (Eberbach Corp., MI, USA).
597 Total biomass (g) was calculated as the sum of dry leaf, stem, root, and root nodule biomass.
598 Carbon and nitrogen content was measured for each organ type through elemental combustion
599 (Costech-4010, Costech, Inc., Valencia, CA, USA) using subsamples of ground and
600 homogenized organ tissue. The ratio of root nodule biomass to root biomass was calculated as an
601 additional indicator of investment toward symbiotic nitrogen fixation.

602 Carbon costs to acquire nitrogen were quantified as the ratio of belowground carbon
603 biomass to total nitrogen biomass (N_{cost} ; gC gN^{-1})⁴⁴. Belowground carbon biomass (C_{bg} ; gC) was
604 calculated as the sum of root carbon biomass and root nodule carbon biomass. Root carbon
605 biomass and root nodule carbon biomass were calculated as the product of the organ biomass and
606 respective organ carbon content. Total nitrogen biomass (N_{wp} ; gN) was calculated as the sum of
607 total leaf, stem, root, and root nodule nitrogen biomass. Leaf, stem, root, and root nodule
608 nitrogen biomass was calculated as the product of the organ biomass and respective organ
609 nitrogen content. This calculation does not account for additional carbon costs associated with
610 respiration, root exudation, or root turnover, and may underestimate carbon costs to acquire
611 nitrogen⁴⁴.

612

613 *Statistical analyses*

614 Uninoculated plants that had substantial root nodule formation (root nodule biomass: root
615 biomass values greater than 0.05 g g^{-1}) were removed from analyses under the assumption that
616 plants were either incompletely sterilized or were colonized by neighboring plants in the
617 chamber. This decision resulted in the removal of sixteen plants from the analysis: two plants in

the elevated CO₂ treatment that received 35 ppm N, three plants in the elevated CO₂ treatment that received 70 ppm N, one plant in the elevated CO₂ treatment that received 210 ppm N, two plants in the elevated CO₂ treatment that received 280 ppm N, two plants in the ambient CO₂ treatment that received 0 ppm N, three plants in the ambient CO₂ treatment that received 70 ppm N, two plants in the ambient CO₂ treatment that received 105 ppm N, and one plant in the ambient CO₂ treatment that received 280 ppm N.

A series of linear mixed-effects models were built to investigate the impacts of CO₂ concentration, nitrogen fertilization, and inoculation on *G. max* leaf nitrogen allocation, gas exchange, whole-plant growth, and investment in nitrogen fixation. All models included CO₂ treatment as a categorical fixed effect, inoculation treatment as a categorical fixed effect, and nitrogen fertilization as a continuous fixed effect, with all possible interaction terms between all three fixed effects also included. Models accounted for climatic differences between chambers across experiment iterations by including a random intercept term that nested the starting chamber rack by CO₂ treatment. Models with this independent variable structure were created for each of the following dependent variables: N_{area} , M_{area} , N_{mass} , Chl_{area} , $A_{\text{net},420}$, $A_{\text{net,growth}}$, $V_{\text{cmax}25}$, $J_{\text{max}25}$, $J_{\text{max}25}:V_{\text{cmax}25}$, $R_{\text{d}25}$, $PNUE_{\text{growth}}$, χ , total leaf area, total biomass, N_{cost} , C_{bg} , N_{wp} , $\%N_{\text{dfa}}$, root nodule biomass: root biomass, root nodule biomass, and root biomass.

Shapiro-Wilk tests of normality were used to assess whether linear mixed-effects models satisfied residual normality assumptions. All models that did not satisfy residual normality assumptions satisfied such assumptions when response variables were fit using either a natural log or square root data transformation (Shapiro-Wilk: $p>0.05$ in all cases). Specifically, models for N_{area} , N_{mass} , Chl_{area} , $A_{\text{net},420}$, $A_{\text{net,growth}}$, $V_{\text{cmax}25}$, $J_{\text{max}25}$, $J_{\text{max}25}:V_{\text{cmax}25}$, $R_{\text{d}25}$, $PNUE_{\text{growth}}$, χ , total leaf area, and N_{cost} each satisfied residual normality assumptions without data transformation. Models for M_{area} , total biomass, and C_{bg} satisfied residual normality assumptions with a natural log data transformation, while models for N_{wp} , root nodule biomass: root biomass, root nodule biomass, root biomass, and $\%N_{\text{dfa}}$ satisfied residual normality assumptions with a square root data transformation.

In all models, we used the ‘lmer’ function in the ‘lme4’ R package⁶⁷ to fit each model and the ‘Anova’ function in the ‘car’ R package⁶⁸ to calculate Type II Wald's χ^2 and determine the significance ($\alpha=0.05$) of each fixed effect coefficient. We used the ‘emmeans’ R package⁶⁹ to conduct post-hoc comparisons using Tukey's tests, where degrees of freedom were approximated

649 using the Kenward-Roger approach⁷⁰. Trendlines and error ribbons representing the 95%
650 confidence intervals were drawn in all figures using ‘emmeans’ outputs across the range in
651 nitrogen fertilization values. All analyses and plots were conducted in R version 4.1.0⁷¹. Model
652 results for χ , C_{bg} , N_{wp} , root nodule biomass: root biomass, root nodule biomass, and root biomass
653 are reported in the *Supplemental Material* (Tables S3-S6; Figs. S3-S6).

654

655 **Conflicts of Interest**

656 The authors declare no conflicts of interest.

657

658 **Acknowledgements**

659 This study is a contribution to the LEMONTREE (Land Ecosystem Models based On New
660 Theory, obseRvations and ExperimEnts) project, funded through the generosity of Eric and
661 Wendy Schmidt by recommendation of the Schmidt Futures programme. EAP acknowledges
662 support from a Texas Tech University Doctoral Dissertation Completion Fellowship and a
663 Botanical Society of America Graduate Student Research Award. This work was also supported
664 by US National Science Foundation awards to NGS (DEB-2045968 and DEB-2217353).

665

666 **Data Availability**

667 All R scripts, data, and metadata are available at <https://doi.org/10.5281/zenodo.10177575> (or on
668 GitHub at: https://github.com/eaperkowski/NxCO2xI_ms_data)

669

670 **Author contributions**

671 EAP conceptualized the study objectives and designed the experiment in collaboration with
672 NGS, collected data, conducted data analysis, and wrote the first manuscript draft. EE assisted
673 with data collection and experiment maintenance. NGS conceptualized study objectives and
674 experimental design with EAP and oversaw experiment progress. All authors provided
675 manuscript feedback and approved the manuscript in its current form for submission to *Nature*
676 *Communications*.

References

1. Davies-Barnard, T. *et al.* Nitrogen cycling in CMIP6 land surface models: progress and limitations. *Biogeosciences* **17**, 5129–5148 (2020).
2. Kou-Giesbrecht, S. *et al.* Evaluating nitrogen cycling in terrestrial biosphere models: a disconnect between the carbon and nitrogen cycles. *Earth Syst. Dyn.* **14**, 767–795 (2023).
3. Prentice, I. C., Liang, X., Medlyn, B. E. & Wang, Y.-P. Reliable, robust and realistic: The three R's of next-generation land-surface modelling. *Atmos. Chem. Phys.* **15**, 5987–6005 (2015).
4. Hungate, B. A., Dukes, J. S., Shaw, M. R., Luo, Y. & Field, C. B. Nitrogen and climate change. *Science (80-.).* **302**, 1512–1513 (2003).
5. Friedlingstein, P. *et al.* Uncertainties in CMIP5 climate projections due to carbon cycle feedbacks. *J. Clim.* **27**, 511–526 (2014).
6. Meyerholt, J., Sickel, K. & Zaehle, S. Ensemble projections elucidate effects of uncertainty in terrestrial nitrogen limitation on future carbon uptake. *Glob. Chang. Biol.* **26**, 3978–3996 (2020).
7. Wieder, W. R., Cleveland, C. C., Smith, W. K. & Todd-Brown, K. Future productivity and carbon storage limited by terrestrial nutrient availability. *Nat. Geosci.* **8**, 441–444 (2015).
8. Zaehle, S. *et al.* Evaluation of 11 terrestrial carbon-nitrogen cycle models against observations from two temperate Free-Air CO₂ Enrichment studies. *New Phytol.* **202**, 803–822 (2014).
9. Poorter, H. *et al.* A meta-analysis of responses of C₃ plants to atmospheric CO₂: dose-response curves for 85 traits ranging from the molecular to the whole-plant level. *New Phytol.* **233**, 1560–1596 (2022).
10. Lee, T. D., Barrott, S. H. & Reich, P. B. Photosynthetic responses of 13 grassland species across 11 years of free-air CO₂ enrichment is modest, consistent and independent of N supply. *Glob. Chang. Biol.* **17**, 2893–2904 (2011).
11. Ainsworth, E. A. & Long, S. P. What have we learned from 15 years of free-air CO₂ enrichment (FACE)? A meta-analytic review of the responses of photosynthesis, canopy properties and plant production to rising CO₂. *New Phytol.* **165**, 351–372 (2005).
12. Ainsworth, E. A. & Rogers, A. The response of photosynthesis and stomatal conductance

- to rising [CO₂]: mechanisms and environmental interactions. *Plant. Cell Environ.* **30**, 258–270 (2007).
13. Curtis, P. S. A meta-analysis of leaf gas exchange and nitrogen in trees grown under elevated carbon dioxide. *Plant, Cell Environ.* **19**, 127–137 (1996).
 14. Drake, B. G., González-Meler, M. A. & Long, S. P. More efficient plants: a consequence of rising atmospheric CO₂? *Annu. Rev. Plant Biol.* **48**, 609–639 (1997).
 15. Pastore, M. A., Lee, T. D., Hobbie, S. E. & Reich, P. B. Strong photosynthetic acclimation and enhanced water-use efficiency in grassland functional groups persist over 21 years of CO₂ enrichment, independent of nitrogen supply. *Glob. Chang. Biol.* **25**, 3031–3044 (2019).
 16. Ainsworth, E. A. *et al.* A meta-analysis of elevated [CO₂] effects on soybean (*Glycine max*) physiology, growth and yield. *Glob. Chang. Biol.* **8**, 695–709 (2002).
 17. LeBauer, D. S. & Treseder, K. Nitrogen limitation of net primary productivity in terrestrial ecosystems is globally distributed. *Ecology* **89**, 371–379 (2008).
 18. Luo, Y. *et al.* Progressive nitrogen limitation of ecosystem responses to rising atmospheric carbon dioxide. *Bioscience* **54**, 731–739 (2004).
 19. Norby, R. J., Warren, J. M., Iversen, C. M., Medlyn, B. E. & McMurtrie, R. E. CO₂ enhancement of forest productivity constrained by limited nitrogen availability. *Proc. Natl. Acad. Sci.* **107**, 19368–19373 (2010).
 20. Reich, P. B. *et al.* Nitrogen limitation constrains sustainability of ecosystem response to CO₂. *Nature* **440**, 922–925 (2006).
 21. Finzi, A. C. *et al.* Progressive nitrogen limitation of ecosystem processes under elevated CO₂ in a warm-temperate forest. *Ecology* **87**, 15–25 (2006).
 22. Liang, J., Qi, X., Souza, L. & Luo, Y. Processes regulating progressive nitrogen limitation under elevated carbon dioxide: a meta-analysis. *Biogeosciences* **13**, 2689–2699 (2016).
 23. Moore, D. J. P. *et al.* Annual basal area increment and growth duration of *Pinus taeda* in response to eight years of free-air carbon dioxide enrichment. *Glob. Chang. Biol.* **12**, 1367–1377 (2006).
 24. Evans, J. R. Photosynthesis and nitrogen relationships in leaves of C₃ plants. *Oecologia* **78**, 9–19 (1989).
 25. Field, C. B. & Mooney, H. A. The photosynthesis-nitrogen relationship in wild plants. in

On the Economy of Plant Form and Function (ed. Givnish, T. J.) 25–55 (Cambridge University Press, 1986).

26. Crous, K. Y., Reich, P. B., Hunter, M. D. & Ellsworth, D. S. Maintenance of leaf N controls the photosynthetic CO₂ response of grassland species exposed to 9 years of free-air CO₂ enrichment. *Glob. Chang. Biol.* **16**, 2076–2088 (2010).
27. Dong, N. *et al.* Leaf nitrogen from first principles: field evidence for adaptive variation with climate. *Biogeosciences* **14**, 481–495 (2017).
28. Dong, N. *et al.* Components of leaf-trait variation along environmental gradients. *New Phytol.* **228**, 82–94 (2020).
29. Dong, N. *et al.* Leaf nitrogen from the perspective of optimal plant function. *J. Ecol.* **110**, 2585–2602 (2022).
30. Paillassa, J. *et al.* When and where soil is important to modify the carbon and water economy of leaves. *New Phytol.* **228**, 121–135 (2020).
31. Peng, Y., Bloomfield, K. J., Cernusak, L. A., Domingues, T. F. & Prentice, I. C. Global climate and nutrient controls of photosynthetic capacity. *Commun. Biol.* **4**, 462 (2021).
32. Waring, E. F., Perkowski, E. A. & Smith, N. G. Soil nitrogen fertilization reduces relative leaf nitrogen allocation to photosynthesis. *J. Exp. Bot.* **74**, 5166–5180 (2023).
33. Harrison, S. P. *et al.* Eco-evolutionary optimality as a means to improve vegetation and land-surface models. *New Phytol.* **231**, 2125–2141 (2021).
34. Wright, I. J., Reich, P. B. & Westoby, M. Least-cost input mixtures of water and nitrogen for photosynthesis. *Am. Nat.* **161**, 98–111 (2003).
35. Prentice, I. C., Dong, N., Gleason, S. M., Maire, V. & Wright, I. J. Balancing the costs of carbon gain and water transport: testing a new theoretical framework for plant functional ecology. *Ecol. Lett.* **17**, 82–91 (2014).
36. Chen, J.-L., Reynolds, J. F., Harley, P. C. & Tenhunen, J. D. Coordination theory of leaf nitrogen distribution in a canopy. *Oecologia* **93**, 63–69 (1993).
37. Maire, V. *et al.* The coordination of leaf photosynthesis links C and N fluxes in C₃ plant species. *PLoS One* **7**, e38345 (2012).
38. Evans, J. R. & Clarke, V. C. The nitrogen cost of photosynthesis. *J. Exp. Bot.* **70**, 7–15 (2019).
39. Smith, N. G. *et al.* Global photosynthetic capacity is optimized to the environment. *Ecol.*

Lett. **22**, 506–517 (2019).

40. Wang, H. *et al.* Towards a universal model for carbon dioxide uptake by plants. *Nat. Plants* **3**, 734–741 (2017).
41. Smith, N. G. & Keenan, T. F. Mechanisms underlying leaf photosynthetic acclimation to warming and elevated CO₂ as inferred from least-cost optimality theory. *Glob. Chang. Biol.* **26**, 5202–5216 (2020).
42. Dong, N. *et al.* Rising CO₂ and warming reduce global canopy demand for nitrogen. *New Phytol.* **235**, 1692–1700 (2022).
43. Brzostek, E. R., Fisher, J. B. & Phillips, R. P. Modeling the carbon cost of plant nitrogen acquisition: Mycorrhizal trade-offs and multipath resistance uptake improve predictions of retranslocation. *J. Geophys. Res. Biogeosciences* **119**, 1684–1697 (2014).
44. Perkowski, E. A., Waring, E. F. & Smith, N. G. Root mass carbon costs to acquire nitrogen are determined by nitrogen and light availability in two species with different nitrogen acquisition strategies. *J. Exp. Bot.* **72**, 5766–5776 (2021).
45. Terrer, C. *et al.* Ecosystem responses to elevated CO₂ governed by plant–soil interactions and the cost of nitrogen acquisition. *New Phytol.* **217**, 507–522 (2018).
46. Smith, N. G. & Dukes, J. S. Plant respiration and photosynthesis in global-scale models: incorporating acclimation to temperature and CO₂. *Glob. Chang. Biol.* **19**, 45–63 (2013).
47. Bytnarowicz, T. A., Funk, J. L., Menge, D. N. L., Perakis, S. S. & Wolf, A. A. Leaf nitrogen affects photosynthesis and water use efficiency similarly in nitrogen-fixing and non-fixing trees. *J. Ecol.* 1–15 (2023).
48. Adams, M. A., Turnbull, T. L., Sprent, J. I. & Buchmann, N. Legumes are different: Leaf nitrogen, photosynthesis, and water use efficiency. *Proc. Natl. Acad. Sci. U. S. A.* **113**, 4098–4103 (2016).
49. Rastetter, E. B. *et al.* Resource optimization and symbiotic nitrogen fixation. *Ecosystems* **4**, 369–388 (2001).
50. Andrews, M. *et al.* Nitrogen fixation in legumes and actinorhizal plants in natural ecosystems: Values obtained using ¹⁵N natural abundance. *Plant Ecol. Divers.* **4**, 117–130 (2011).
51. McCulloch, L. A. & Porder, S. Light fuels while nitrogen suppresses symbiotic nitrogen fixation hotspots in neotropical canopy gap seedlings. *New Phytol.* **231**, 1734–1745

(2021).

52. Friel, C. A. & Friesen, M. L. Legumes modulate allocation to rhizobial nitrogen fixation in response to factorial light and nitrogen manipulation. *Front. Plant Sci.* **10**, 1316 (2019).
53. Taylor, B. N. & Menge, D. N. L. Light regulates tropical symbiotic nitrogen fixation more strongly than soil nitrogen. *Nat. Plants* **4**, 655–661 (2018).
54. Rogers, A. *et al.* A roadmap for improving the representation of photosynthesis in Earth system models. *New Phytol.* **213**, 22–42 (2017).
55. Luo, X. *et al.* Global variation in the fraction of leaf nitrogen allocated to photosynthesis. *Nat. Commun.* **12**, 4866 (2021).
56. Kattge, J., Knorr, W., Raddatz, T. & Wirth, C. Quantifying photosynthetic capacity and its relationship to leaf nitrogen content for global-scale terrestrial biosphere models. *Glob. Chang. Biol.* **15**, 976–991 (2009).
57. Walker, A. P. *et al.* The relationship of leaf photosynthetic traits - V_{cmax} and J_{max} - to leaf nitrogen, leaf phosphorus, and specific leaf area: a meta-analysis and modeling study. *Ecol. Evol.* **4**, 3218–3235 (2014).
58. Poorter, H., Böhler, J., Van Dusschoten, D., Climent, J. & Postma, J. A. Pot size matters: A meta-analysis of the effects of rooting volume on plant growth. *Funct. Plant Biol.* **39**, 839–850 (2012).
59. Hoagland, D. R. & Arnon, D. I. The water-culture method for growing plants without soil. *Calif. Agric. Exp. Stn.* **347** **347**, 1–32 (1950).
60. Saathoff, A. J. & Welles, J. Gas exchange measurements in the unsteady state. *Plant Cell Environ.* **44**, 3509–3523 (2021).
61. Duursma, R. A. Plantecophys - an R package for analysing and modelling leaf gas exchange data. *PLoS One* **10**, e0143346 (2015).
62. Farquhar, G. D., von Caemmerer, S. & Berry, J. A. A biochemical model of photosynthetic CO_2 assimilation in leaves of C_3 species. *Planta* **149**, 78–90 (1980).
63. Bernacchi, C. J., Singsaas, E. L., Pimentel, C., Portis, A. R. & Long, S. P. Improved temperature response functions for models of Rubisco-limited photosynthesis. *Plant, Cell Environ.* **24**, 253–259 (2001).
64. Katabuchi, M. LeafArea: An R package for rapid digital analysis of leaf area. *Ecol. Res.* **30**, 1073–1077 (2015).

65. Barnes, J. D., Balaguer, L., Manrique, E., Elvira, S. & Davison, A. W. A reappraisal of the use of DMSO for the extraction and determination of chlorophylls a and b in lichens and higher plants. *Environ. Exp. Bot.* **32**, 85–100 (1992).
66. Wellburn, A. R. The spectral determination of chlorophylls a and b, as well as total carotenoids, using various solvents with spectrophotometers of different resolution. *J. Plant Physiol.* **144**, 307–313 (1994).
67. Bates, D., Mächler, M., Bolker, B. & Walker, S. Fitting linear mixed-effects models using lme4. *J. Stat. Softw.* **67**, 1–48 (2015).
68. Fox, J. & Weisberg, S. *An R companion to applied regression*. (Sage, 2019).
69. Lenth, R. emmeans: estimated marginal means, aka least-squares means. at (2019).
70. Kenward, M. G. & Roger, J. H. Small sample inference for fixed effects from restricted maximum likelihood. *Biometrics* **53**, 983 (1997).
71. R Core Team. R: A language and environment for statistical computing. at <https://www.r-project.org/> (2021).